



# Insulin increases glomerular filtration barrier permeability through PKGI $\alpha$ -dependent mobilization of BK<sub>Ca</sub> channels in cultured rat podocytes

Agnieszka Piwkowska<sup>a,\*</sup>, Dorota Rogacka<sup>a</sup>, Irena Audzeyenka<sup>a</sup>, Małgorzata Kasztan<sup>b</sup>, Stefan Angielski<sup>a</sup>, Maciej Jankowski<sup>a,c</sup>

<sup>a</sup> Mossakowski Medical Research Centre, Polish Academy of Sciences, Laboratory of Molecular and Cellular Nephrology, Gdańsk, Poland

<sup>b</sup> Medical University of Gdańsk, Department of Therapy Monitoring and Pharmacogenetics, Poland

<sup>c</sup> Medical University of Gdańsk, Department of Clinical Chemistry, Poland

## ARTICLE INFO

### Article history:

Received 8 January 2015

Received in revised form 23 April 2015

Accepted 27 April 2015

Available online 4 May 2015

### Keywords:

Insulin

Filtration barrier permeability

Podocyte

Large-conductance Ca<sup>2+</sup>-activated K<sup>+</sup> channels

Constriction apparatus

## ABSTRACT

Podocytes are highly specialized cells that wrap around glomerular capillaries and comprise a key component of the glomerular filtration barrier. They are uniquely sensitive to insulin; like skeletal muscle and fat cells, they exhibit insulin-stimulated glucose uptake and express glucose transporters. Podocyte insulin signaling is mediated by protein kinase G type I (PKGI), and it leads to changes in glomerular permeability to albumin. Here, we investigated whether large-conductance Ca<sup>2+</sup>-activated K<sup>+</sup> channels (BK<sub>Ca</sub>) were involved in insulin-mediated, PKGI $\alpha$ -dependent filtration barrier permeability.

Insulin-induced glomerular permeability was measured in glomeruli isolated from Wistar rats. Transepithelial albumin flux was measured in cultured rat podocyte monolayers. Expression of BK<sub>Ca</sub> subunits was detected by RT-PCR. BK<sub>Ca</sub>, PKGI $\alpha$ , and upstream protein expression were examined in podocytes with Western blotting and immunofluorescence. The BK<sub>Ca</sub>-PKGI $\alpha$  interaction was assessed with co-immunoprecipitation.

RT-PCR showed that primary cultured rat podocytes expressed mRNAs that encoded the pore-forming  $\alpha$  subunit and four accessory  $\beta$  subunits of BK<sub>Ca</sub>. The BK<sub>Ca</sub> inhibitor, iberiotoxin (ibTX), abolished insulin-dependent glomerular albumin permeability and PKGI-dependent transepithelial albumin flux. Insulin-evoked albumin permeability across podocyte monolayers was also blocked with BK<sub>Ca</sub> siRNA. Moreover, ibTX blocked insulin-induced disruption of the actin cytoskeleton and changes in the phosphorylation of PKG target proteins, MYPT1 and RhoA. These results indicated that insulin increased filtration barrier permeability through mobilization of BK<sub>Ca</sub> channels via PKGI in cultured rat podocytes. This molecular mechanism may explain podocyte injury and proteinuria in diabetes.

© 2015 Elsevier B.V. All rights reserved.

## 1. Introduction

Podocytes are highly specialized cells that wrap around glomerular capillaries, and they comprise a key component of the glomerular filtration barrier. Podocyte damage leads to a retraction of the foot processes, and proteinuria ensues [1].

Podocytes consist of three morphologically and functionally different segments: a cell body, major processes, and foot processes. The podocyte cell body gives rise to primary processes that branch into foot processes; in turn, the foot processes of neighboring podocytes

establish a highly branched, interdigitating pattern known as the slit diaphragm [1]. The slit diaphragm represents a signaling platform that regulates podocyte function and includes many proteins, including nephrin, podocin, Neph1, CD2AP, TRPC6, BK<sub>Ca</sub>, and actin [2–5].

Podocytes express proteins that are characteristic of the smooth muscle cell contractile system [6,7]. The presence of F-actin, myosin, and  $\alpha$ -actinin in foot processes was proposed to facilitate glomerular adaptation to changes in pressure gradients; rearrangements of these proteins can modify the surface area for filtration. Podocytes also express receptors for factors that regulate contraction and relaxation; this suggested that podocyte function may be regulated by vasoactive hormones and autocrine/paracrine factors [8,9]. Moreover, mechanical stress induces F-actin reorganization. Podocyte processes become thin and elongated in response to mechanical stress. The podocyte cell body size is smaller in stressed compared to unstressed conditions. Podocytes cultured *in vitro* exhibit a unique ability to reorganize the actin cytoskeleton, which depends on Ca<sup>2+</sup> influx and Rho kinase.

**Abbreviations:** BK<sub>Ca</sub>, large-conductance Ca<sup>2+</sup>-activated K<sup>+</sup> channels; PKGI $\alpha$ , protein kinase G type I $\alpha$ ; MLC, myosin light chain; MLCP, myosin light chain phosphatase; MLCK, myosin light chain kinase; MYPT1, myosin phosphatase target subunit 1

\* Corresponding author at: Laboratory of Molecular and Cellular Nephrology, Mossakowski Medical Research Center Polish Academy of Sciences, Dębinki 7, 80-211 Gdańsk, Poland. Tel.: +48 58 3492789; fax: +48 58 3492784.

E-mail address: [apiwkowska@imdik.pan.pl](mailto:apiwkowska@imdik.pan.pl) (A. Piwkowska).

This reorganization results in the formation of radial stress fibers connected to an actin-rich center. Thus, podocytes can be regarded as intrinsically mechanosensitive cells [8]. In addition, hormonal regulation of podocytes affects the size-selectivity of the filtration barrier. This regulation may be similar to that of smooth muscle cells. The size-selective properties of podocytes are also regulated by cGMP-dependent changes in proteins, like protein kinase G type I alpha (PKG $\alpha$ ), which may regulate the cytoskeleton and slit diaphragm.

The PKG $\alpha$  isoform stimulates myosin light-chain phosphatase (MLCP) activity by phosphorylating its regulatory subunit, MYPT1, at Ser 695 and Ser 852 [10,11]. Increased MLCP activity reduces the level of MLC phosphorylation and causes relaxation [12]. Moreover, PKG $\alpha$  opposes the inhibitory effect of RhoA/ROCK on MLCP activity. PKG $\alpha$  directly inhibits RhoA by phosphorylation at Ser188 [13], and it directly phosphorylates large-conductance Ca<sup>2+</sup>-activated K<sup>+</sup> channels (BK<sub>Ca</sub>) [14].

BK<sub>Ca</sub> channels are a unique class of ion channel; they couple intracellular chemical and electrical signals in podocytes [4,15]. These channels interact with podocyte proteins that are functionally connected to the foot process cytoskeleton, including nephrin [15], the nephrin-like protein, Neph1 [16], synaptopodin [17], and the transient receptor potential cation channel, TRPC6 [18]. The binding of mechanosensitive TRPC6 to BK<sub>Ca</sub> channels may allow the activation of BK<sub>Ca</sub> channels by Ca<sup>2+</sup> influx during podocytes stretch [18]. Moreover, an intact actin cytoskeleton is required for normal expression of BK<sub>Ca</sub> channels on the podocyte cell surface [19].

Growing evidence has suggested that insulin plays important roles in podocyte metabolism and function [20]. We previously demonstrated that insulin increased the activation of PKG $\alpha$  subunits, which led to podocyte dysfunction [21]. We found relationships between PKG $\alpha$  activation, oxidative stress, actin reorganization, and changes in the permeability of the filtration layer to albumin [22]. Other studies showed that insulin stimulated the surface expression of BK<sub>Ca</sub> channel pore-forming subunits (Slo1 proteins) in mouse podocytes. This expression was accompanied by an increase in BK<sub>Ca</sub> channel activity [19]. In the present study, we investigated whether BK<sub>Ca</sub> was involved in insulin-mediated, PKG $\alpha$ -dependent regulation of filtration barrier permeability.

## 2. Materials and methods

### 2.1. Isolation of renal glomeruli

Rat kidneys were removed and placed in ice-cold PBS, pH 7.4, supplemented with 5.6 mM glucose. Glomeruli were isolated with a gradual sieving technique [23]. Briefly, the renal capsule was removed, and the cortex was minced with a razor blade to a paste-like consistency. This was strained through a steel sieve with a pore size of 250  $\mu$ m. The material that passed through this sieve was suspended in ice-cold PBS and then passed through two consecutive steel sieves (120 and 70  $\mu$ m pores). The glomeruli retained on top of the 70  $\mu$ m sieve were washed off with ice-cold PBS and resuspended in ice-cold PBS buffer. The final suspension consisted of decapsulated glomeruli devoid of afferent and efferent arterioles. The tubular contamination was less than 5%, assessed under the light microscope. The entire procedure was carried out in an ice bath and it was completed in no more than 1 h.

### 2.2. Preparation and culture of rat podocytes

All experiments were approved by the local ethics committee (No. 11/2007). Female Wistar rats weighing 100–120 g were anesthetized with thiopental (70 mg per kg body weight, i.p.). The kidneys were excised and minced with a scalpel, then pressed through a system of sieves with decreasing pore diameters (160, 106, and 53  $\mu$ m). The final material comprised glomeruli suspended in RPMI 1640 supplemented with 10% FBS, 100 U/mL penicillin, and 100 mg/mL streptomycin. The

glomeruli were plated in 75 cm<sup>2</sup>, type I collagen-coated culture flasks (Becton Dickinson Labware, Beckton, UK), and maintained at 37 °C in an atmosphere of 95% air and 5% CO<sub>2</sub> for 5–7 days. The outgrowing podocytes were trypsinized and passed through sieves with 33- $\mu$ m pores to remove the remaining glomerular cores. The suspended podocytes were seeded in culture flasks and cultivated at 37 °C in an atmosphere of 95% air and 5% CO<sub>2</sub>. Experiments were performed with podocytes that were cultivated for 12–20 days. The podocyte phenotype and cell viability were determined as described previously with immunocytochemical methods. Cell phenotype was determined with podocyte-specific antibodies against Wilm's tumor-1 protein, WT-1 (Biotrend Koeln, Germany) and synaptopodin (Progen, Heidelberg, Germany). Cell viability was determined by detecting lactate dehydrogenase leakage.

### 2.3. Western blot analysis

Podocytes were suspended in lysis buffer (1% Nonidet P-40, 20 mM Tris, 140 mM NaCl, 2 mM EDTA, 10% glycerol) in the presence of a protease inhibitor cocktail (Sigma-Aldrich), and homogenized at 4 °C by scraping. The cell homogenates were centrifuged at 9500  $\times$  g for 20 min at 4 °C. Supernatant proteins (20  $\mu$ g) were separated on an SDS-polyacrylamide gel (10%) and electrotransferred to a nitrocellulose membrane. The membrane was blocked for 1.5 h with Tris-buffered saline (TBS) (20 mM Tris-HCl, 140 mM NaCl, 0.01% NaN<sub>3</sub>) containing 3% non-fat dry milk. Then, membranes were washed with TBS containing 0.1% Tween-20 and 0.1% bovine serum albumin (BSA). Next, membranes were incubated overnight at 4 °C with primary antibodies diluted in TBS containing 0.05% Tween-20 and 1% BSA. The following primary antibodies were used: anti-p-RhoA (Ser188) (1:400, Sigma-Aldrich), anti-RhoA (1:400, Santa Cruz Biotechnology), anti-PKG $\alpha$  (1:400, Santa Cruz Biotechnology), anti-MYPT1 (1:400, Santa Cruz Biotechnology), anti-p-MYPT1 (Ser-695) (1:400, Santa Cruz Biotechnology), anti-Slo1 (1:1000, Abcam), anti-MaxiK $\beta$  (1:400, Santa Cruz Biotechnology), and anti-actin (1:3000, Sigma-Aldrich). To detect primary antibodies bound to proteins on the immunoblot, the membrane was incubated for 2 h with the appropriate alkaline phosphatase (AP)-conjugated secondary antibodies (goat anti-rabbit IgG-AP, goat anti-mouse IgG-AP, or goat anti-rabbit IgG-AP, Santa Cruz Biotechnology). The protein bands were detected with the colorimetric 5-bromo-4-chloro-3-indolylphosphate/nitroblue tetrazolium (BCIP/NBT) system. The band density was measured quantitatively with the Quantity One program (Bio-Rad). Protein content was measured with the Lowry method.

### 2.4. Immunofluorescence

Podocytes were seeded on coverslips coated with type-I collagen (Becton Dickinson Labware, Beckton, UK) and cultured in RPMI 1640 supplemented with 10% FBS. Then, cells were fixed in PBS containing 2% formaldehyde for 10 min at room temperature. Next, the coverslips were placed on ice, and the cells were permeabilized by adding 0.3% Triton-X 100 for 3–4 min, and then, cells were blocked with a PBSB solution (PBS containing 2% FBS, 2% BSA, and 0.2% fish gelatin) for 60 min. After blocking, cells were incubated with anti-PKG $\alpha$  and anti-Slo1 antibodies in PBSB (1:100) at 4 °C for 1 h. Non-specific staining was evaluated by substituting the primary antibodies with PBSB. Next, cells were washed three times with cold PBS and incubated for 45 min with secondary anti-mouse antibodies conjugated with Alexa Fluor 488 (1:100) or anti-goat antibodies (1:100) conjugated with Cy3. After three 5-min washes, the coverslips were attached to slides with Mowiol 4-88 diluted in glycerol-PBS (1:3 v:v), and the cells were viewed with a confocal laser scanning microscope (Olympus FluoView FV10i) or with a fluorescence microscope (Olympus IX51).

F-actin network was labeled and visualized by fluorescence microscopy as described by Pubill et al. with minor modifications [24].

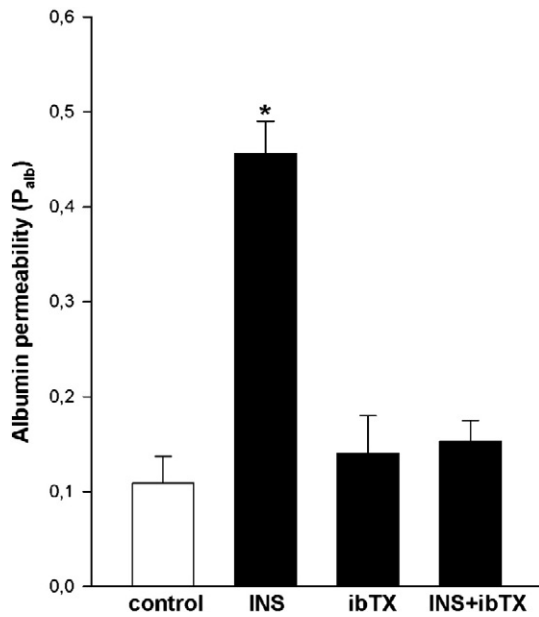


**Fig. 1.** BK<sub>Ca</sub> inhibition with iberiotoxin (ibTX) reduced insulin-stimulated glomerular albumin permeability. Glomerular albumin permeability (P<sub>alb</sub>) was measured in isolated glomeruli exposed to an oncotic gradient with or without insulin (INS, 300 nM, 5 min) and iberiotoxin (ibTX, 20 nM, 20 min). Control glomeruli received the same treatments, but without an oncotic gradient (5% bovine serum albumin inside and outside). The values represent the mean  $\pm$  SEM (n = 12–14 glomeruli from four rats), \*P < 0.05 compared to control.

Digitized fluorescence images of F-actin network were used to generate fluorescence intensity profiles (from basal membrane to nucleus) using the CellSens image software. To normalize the fluorescence intensity profiles originating from different cells, we expressed the fluorescence intensity of X-axis pixels in distance of 1  $\mu$ m as the percentage of the mean value of the fluorescence intensity for the total X-axis and the cell membrane was positioned at point 0. Fluorescence values of each profile were expressed as a percentage of the mean fluorescence value of the corresponding profile.

### 2.5. Permeability assay

Transepithelial permeability to albumin was evaluated by measuring the diffusion of FITC-labeled BSA (Sigma) across the podocyte monolayer, as described by Oshima et al., with minor modifications [25]. Rat podocytes ( $1 \times 10^5$  cells/cm<sup>2</sup>) were seeded on type IV collagen-coated Cell Culture Inserts (3- $\mu$ m membrane pore size, 0.32 cm<sup>2</sup> membrane surface area, BD Biosciences). Inserts were placed in 24-well plates, and the cells were allowed to differentiate for one

week. Cells were used for experiments between post-seeding days 7 and 15. Before use in experiments, the podocytes were washed twice with PBS and medium on both sides of the insert, and the medium was replaced with serum-free RPMI 1640 medium (SFM). After 2 h, the medium in the upper compartment was replaced with 0.3 mL fresh SFM, and that in the lower compartment was replaced with 1.5 mL SFM containing 1 mg/mL FITC-albumin. After 1 h incubation, 200  $\mu$ L of the solution in the upper chamber was transferred to a 96-well plate, and the absorbance of the FITC-albumin was determined by measuring absorbance at 490 nm with a plate spectrophotometer (BioTek EL808).

### 2.6. Glomerular permeability to albumin in vitro

The volume response of glomerular capillaries to an oncotic gradient generated by defined concentrations of albumin was measured as described previously [26]. Isolated glomeruli were allowed to fix to glass coverslips coated with poly-L-lysine (1 mg/mL) and incubated in medium containing 5% BSA, insulin (300 nM, 5 min), and apocynin (100  $\mu$ M) for 15 min at 37  $^{\circ}$ C. Afterwards, the insulin and/or apocynin were washed out with 5% BSA medium. The initial incubation medium was replaced with a medium that contained 1% BSA to produce an oncotic gradient across the glomerular capillary wall. Control glomeruli were treated with equivalent volumes of buffer that contained 5% BSA (no oncotic gradient). The glomerular volume responses were recorded with videomicroscopy (Olympus microscope IX51) before and 1 min after the test reagents were added. Glomerular volume (V) was calculated from the surface area (S) of the glomerulus with the formula:  $V = 3/4\pi (S/\pi)^{3/4}$  with cellSens Dimension software (Olympus). There is a direct relationship between the increase in glomerular volume ( $\Delta V$ ) calculated as  $(V_{\text{final}} - V_{\text{initial}})/V_{\text{initial}}$  and the oncotic gradient ( $\Delta \Pi$ ) applied across the capillary wall. This principle was used to calculate the reflection coefficient of albumin ( $\sigma_{\text{alb}}$ ), defined as the ratio of  $\Delta V$ s in the presence (experimental) and absence (control) of an oncotic gradient:

$$\sigma_{\text{alb}} = \Delta V_{\text{experimental}} / \Delta V_{\text{control}}$$

The reflection coefficient of albumin was used to calculate the glomerular capillary permeability to albumin (convective P<sub>alb</sub> =  $1 - \sigma_{\text{alb}}$ ), which describes the movement of albumin consequent to water flow. At least ten glomeruli isolated from three or more rats were studied in each experiment.

### 2.7. RNA interference and cell transfection

Small interference RNA (siRNA) that targeted the BK<sub>Ca</sub> beta subunit (MaxiK $\beta$ ) mRNA transcript and a nonsilencing siRNA (scrambled siRNA, negative control) were obtained from Santa Cruz Biotechnology.

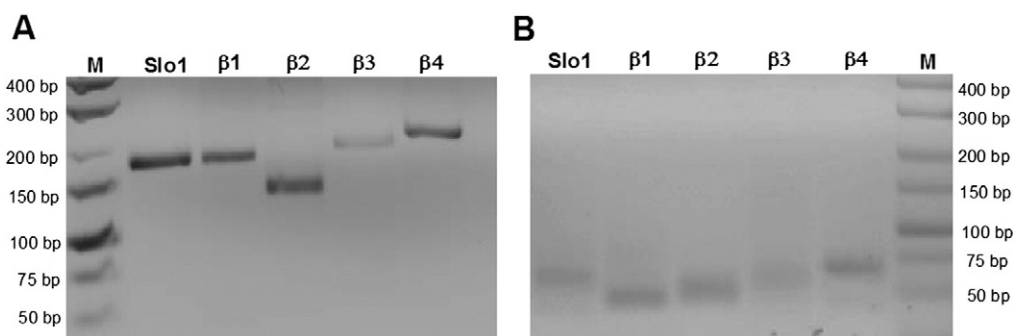


**Fig. 2.** Identification of BK<sub>Ca</sub> channel subunit mRNA in cultured rat podocytes. (A) RT-PCR results show expression levels of Slo1 and  $\beta$ 1 to  $\beta$ 4 subunits, as indicated, in cultured rat podocytes. The predicted sizes of the amplicons were 171, 170, 133, 186, and 202 bp for Slo1 and  $\beta$ 1–4, respectively. (B) Negative control shows PCR products from the mixture without reverse transcriptase. M, molecular weight ladder.

Podocytes were seeded at a density of  $9 \times 10^4$  cells/well in six-well plates coated with type-I collagen (Becton Dickinson Labware, Beckton, UK) and cultured in RPMI 1640 supplemented with 10% FBS. One day before transfection, the culture medium was removed, and cells were cultivated in antibiotic-free RPMI 1640 supplemented with 10% FBS. The siRNA was transfected into cells with a siRNA Transfection Reagent (Santa Cruz Biotechnology), according to the manufacturer's instructions. Briefly, MaxiK $\beta$  siRNAs or scrambled siRNAs were diluted in transfection medium (final concentration, 80 nM), mixed with siRNA Transfection Reagent, and incubated for 30 min at room temperature. This transfection mixture was added to the transfection medium, mixed gently, and added to the cells. After 7 h, a growth medium was added that contained 2-fold higher concentrations of FBS and

antibiotics. Then, the cells were incubated for an additional 24 h. After transfection, gene silencing was monitored at the protein level by Western blotting.

### 2.8. Preparation of the membrane and cytosolic fractions

Podocytes were washed twice with ice-cold PBS and homogenized in a lysis buffer (30 mM Tris, pH 7.5, 10 mM EGTA, 5 mM EDTA, 1 mM DTT, 250 mM sucrose) in the presence of a protease inhibitor cocktail (Sigma-Aldrich). The lysates were centrifuged at  $9500 \times g$  for 10 min at 4 °C, and the supernatant was ultracentrifuged at  $60,000 \times g$  for 30 min at 4 °C. Afterwards, the supernatant was used as the cytosolic fraction and the pellet was resuspended in lysis buffer (without

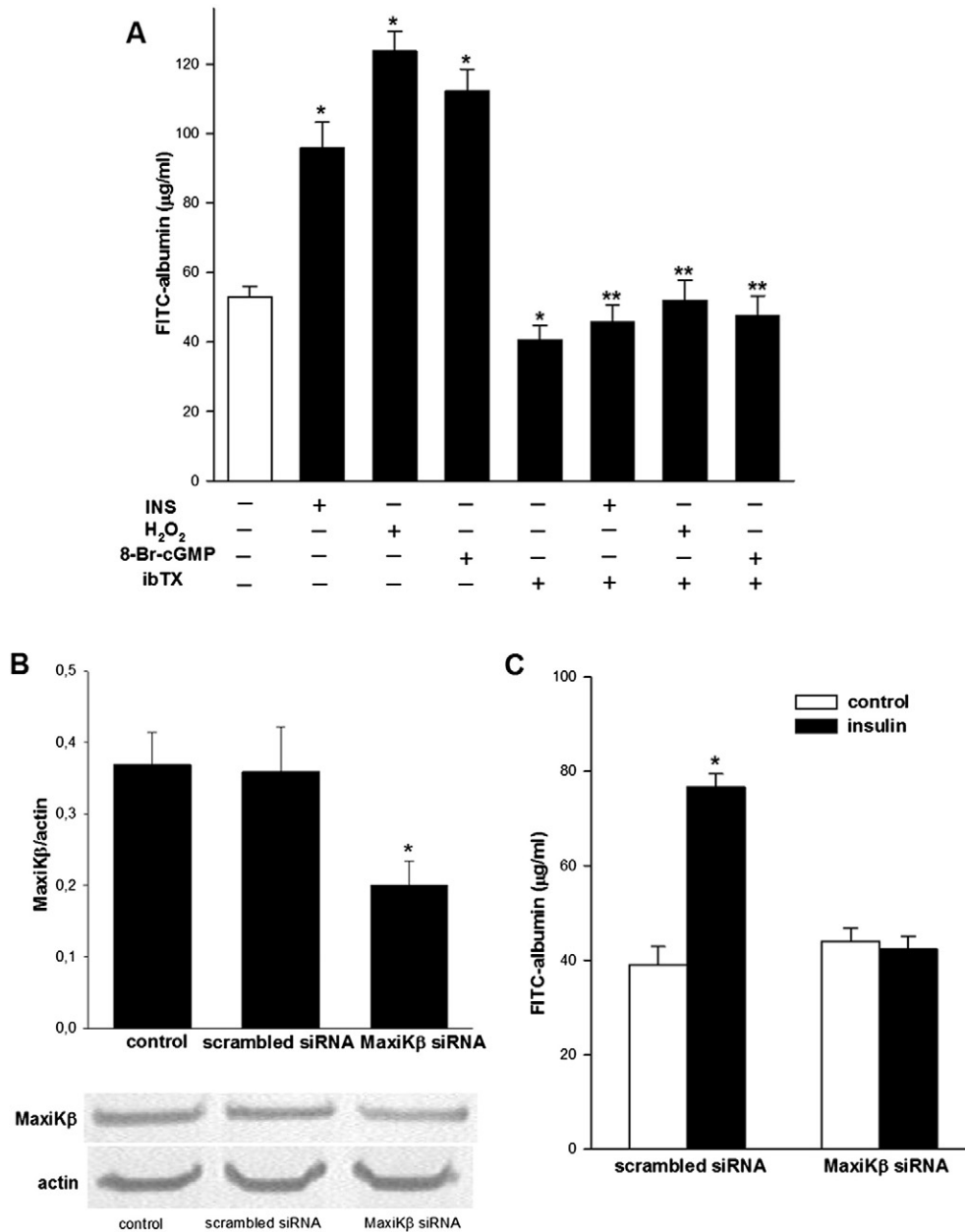


**Fig. 3.** Insulin increases permeability to albumin in cultured rat podocyte monolayers via PKG $\alpha$ -dependent BK $\text{Ca}$  activation. (A) The effects of insulin (INS, 300 nM, 5 min), PKG activators (H<sub>2</sub>O<sub>2</sub> and 8-Br-cGMP, 100  $\mu$ M, 5 min), and BK $\text{Ca}$  inhibitor, iberiotoxin (ibTX, 20 nM, 20 min), on albumin permeability across a podocyte monolayer. Results from four experiments are shown as the mean  $\pm$  SEM; \* $P$  < 0.05 compared to control, \*\* $P$  < 0.05 compared to the appropriate control with insulin or PKG activators. (B, upper panel) Effects of small-interfering RNA (siRNA) that targeted MaxiK $\beta$  subunit transcripts in cultured rat podocytes. Densitometry was performed to evaluate the expression of MaxiK $\beta$  protein, normalized to the expression of actin. Controls were transfected with a scrambled siRNA. Values are the means  $\pm$  SEM ( $n$  = 4). \* $P$  < 0.05 vs. other groups. (Lower panel) Representative immunoblots of homogenates from transfected podocytes show MaxiK $\beta$  and actin expression. (C) The effects of downregulating MaxiK $\beta$  on podocyte albumin permeability in the presence of insulin. Values represent the means  $\pm$  SEM of four independent experiments. \* $P$  < 0.05 compared to control.

sucrose) and solubilized with 1% Triton X-100 for use as the membrane fraction. The expression of the Slo1 subunit protein in membrane and cytosolic fractions was examined by Western blot analysis.

### 2.9. Real-time PCR analysis

Total RNA was isolated from cultured podocytes by adding the TRI Reagent (Sigma-Aldrich) and performing chloroform/isopropanol extraction. The quantity of isolated RNA was determined with spectrometry (NanoDrop 2000 UV-Vis, Thermo Scientific). The RNA was considered pure when the A260/A280 ratio was 1.8 to 2.2. Next, the

RNA solution was treated with deoxyribonuclease I (DNase I) (Sigma-Aldrich) to eliminate possible contaminating DNA.

Reverse transcription was performed with 700 ng of RNA (DNase treated) and 100 U of M-MLV Reverse Transcriptase (Promega) in a mixture of M-MLV Reaction Buffer, 0.2 mM dNTPs, 10 mM DTT, 0.25  $\mu$ g Primer p(dT)15 (Roche), and 8 U of RNase Inhibitor (EURx). Reverse transcription was allowed to proceed for 1 h at 42 °C, and then, the reaction was heated for 5 min at 95 °C.

Real-time PCR was performed with a Roche LightCycler® 480 system to evaluate the mRNA expression of the alpha pore-forming gene, *Kcna1*, and the four genes that encode components of the BK<sub>Ca</sub> beta

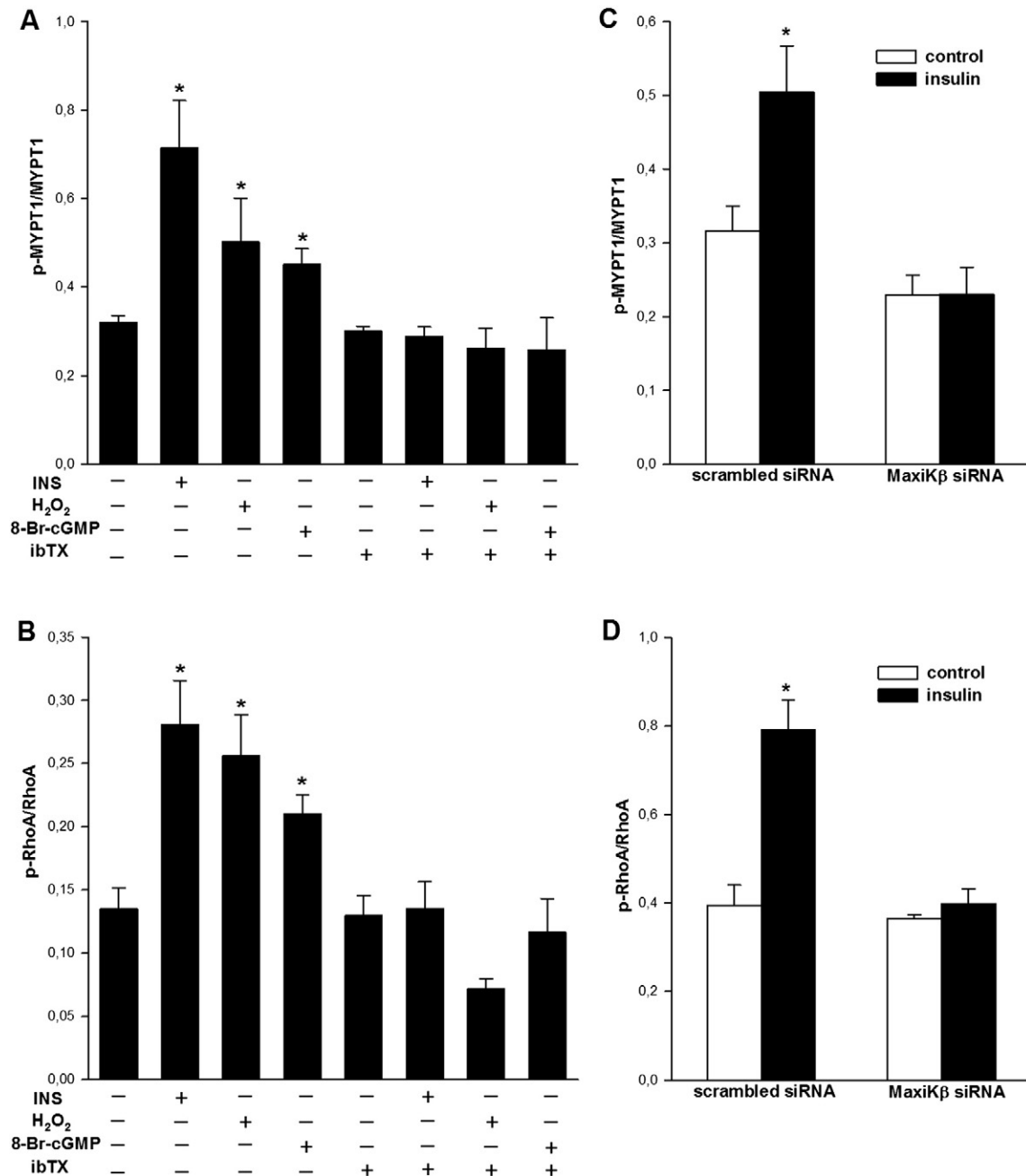


**Fig. 4.** Insulin increases phosphorylation of the myosin-binding subunit of myosin phosphatase I (MYPT1) and phosphorylation of RhoA kinase in cultured rat podocytes via PKG $\alpha$ -dependent BK<sub>Ca</sub> activation. Cells were stimulated with insulin (INS, 300 nM, 5 min) or PKG activators (H<sub>2</sub>O<sub>2</sub> and 8-Br-cGMP, 100  $\mu$ M, 5 min) in the presence or absence of the BK<sub>Ca</sub> inhibitor, iberiotoxin (ibTX, 20 nM, 20 min pre-incubation). Proteins (20  $\mu$ g) were separated by SDS-PAGE, immunoblotted with anti-MYPT1, anti-phospho-MYPT1 (Ser 695), anti-RhoA, and anti-phospho-RhoA (Ser 188) antibodies, and visualized with an alkaline phosphatase-dependent reaction. Densitometric quantification of the corresponding bands was performed, and values are reported as the ratios of band intensities (A) for p-MYPT1 (Ser 695) to MYPT1 and (B) for p-RhoA to RhoA. The values shown represent the mean  $\pm$  SEM of four independent experiments. \*P < 0.05 compared to untreated cells. (C, D) The effects of downregulating MaxiK $\beta$  on (C) MYPT1 and (D) RhoA kinase phosphorylation in the presence of insulin. The values shown represent the means  $\pm$  SEM of four independent experiments. \*P < 0.05 compared to control.

subunit, *Kcnm*β1, *Kcnm*β2, *Kcnm*β3, and *Kcnm*β4. The total reaction mix (final volume 20 μL) contained ~70 ng of cDNA, 1 × LightCycler® FastStart DNA Master SYBR Green I (Roche), 4 mM MgCl<sub>2</sub>, and 0.5 μM each of sense and antisense intron-spanning primers. The PCR conditions were: pre-incubation 10 min at 95 °C, then 35 cycles of: denaturation for 10 s at 95 °C, annealing for 5 s at 60–62 °C, and elongation for 18 s at 72 °C. The primer sequences were: 5'-GCC AGG CAG ATG GTA CTC TCA A-3' (forward), 5'-CAA GGG CAC CAA TGCT GA GA-3' (reverse) for *Kcnm*α1; 5'-ACC ACT GTG CTG CCC CTC TA-3' (forward), 5'-ATA CAG CAT GGC CCA TCT GC-3' (reverse) for *Kcnm*β1; 5'-CGC TCG TAC ATG CAG AGT GT-3' (forward), 5'-GCA GGC AAG GGT ACT GAG AG-3' (reverse) for *Kcnm*β2; 5'-CTT CCA TCG AGC GCT GGT GA-3' (forward), 5'-GCA AAG TCC AGC CAA TCA TCT GC-3' (reverse) for *Kcnm*β3; and 5'-ATG GCG AAG CTC AGG GTG TC-3' (forward), 5'-ACT CGA ACA CCT CGC CGA TC-3' (reverse) for *Kcnm*β4. The PCR products were verified on melting curve plots and in 2.5% agarose gels stained with ethidium bromide.

### 2.10. Immunoprecipitation

Cell extracts were pre-cleared with mouse IgG plus Protein A/G-PLUS Agarose at 4 °C for 1 h. Then, extracts were incubated with a primary antibody plus Protein A/G-PLUS Agarose at 4 °C overnight. The agarose beads were washed gently once with lysis buffer. Proteins were eluted from the beads by adding SDS loading buffer. Then, the mixture was boiled for 5 min and subjected to Western blot analysis.

### 2.11. Statistical analysis

Statistical analyses were performed with one-way ANOVAs followed by the Student–Newman–Keuls test to determine significance. Values are reported as the mean ± SEM. Significance was set at  $P < 0.05$ .

## 3. Results

### 3.1. Iberitoxin reduces insulin-stimulated glomerular albumin permeability in Wistar rats

In the presence of 300 nM insulin, significant increases were observed in the albumin permeability (Palb) of isolated glomeruli ( $0.466 \pm 0.03$ ,  $n = 12$  vs. control  $0.11 \pm 0.03$ ,  $n = 12$ ;  $P < 0.001$ ), within 5 min of incubation (Fig. 1). This effect was prevented by the BK<sub>Ca</sub> inhibitor, iberitoxin (20 nM, 20 min preincubation); inhibition resulted in a Palb of  $0.15 \pm 0.02$  ( $n = 12$ ).

### 3.2. Cultured rat podocytes express mRNA for the Ca<sup>2+</sup>-activated K<sup>+</sup> channel

We performed RT-PCR with total RNA extracted from primary cultured rat podocytes to evaluate mRNA expression of the pore forming α subunit (Slo1) and four accessory beta subunits of BK<sub>Ca</sub> (Fig. 2A) PCR reactions without reverse transcriptase showed no amplification product; this excluded amplification of contaminating DNA (Fig. 2B).

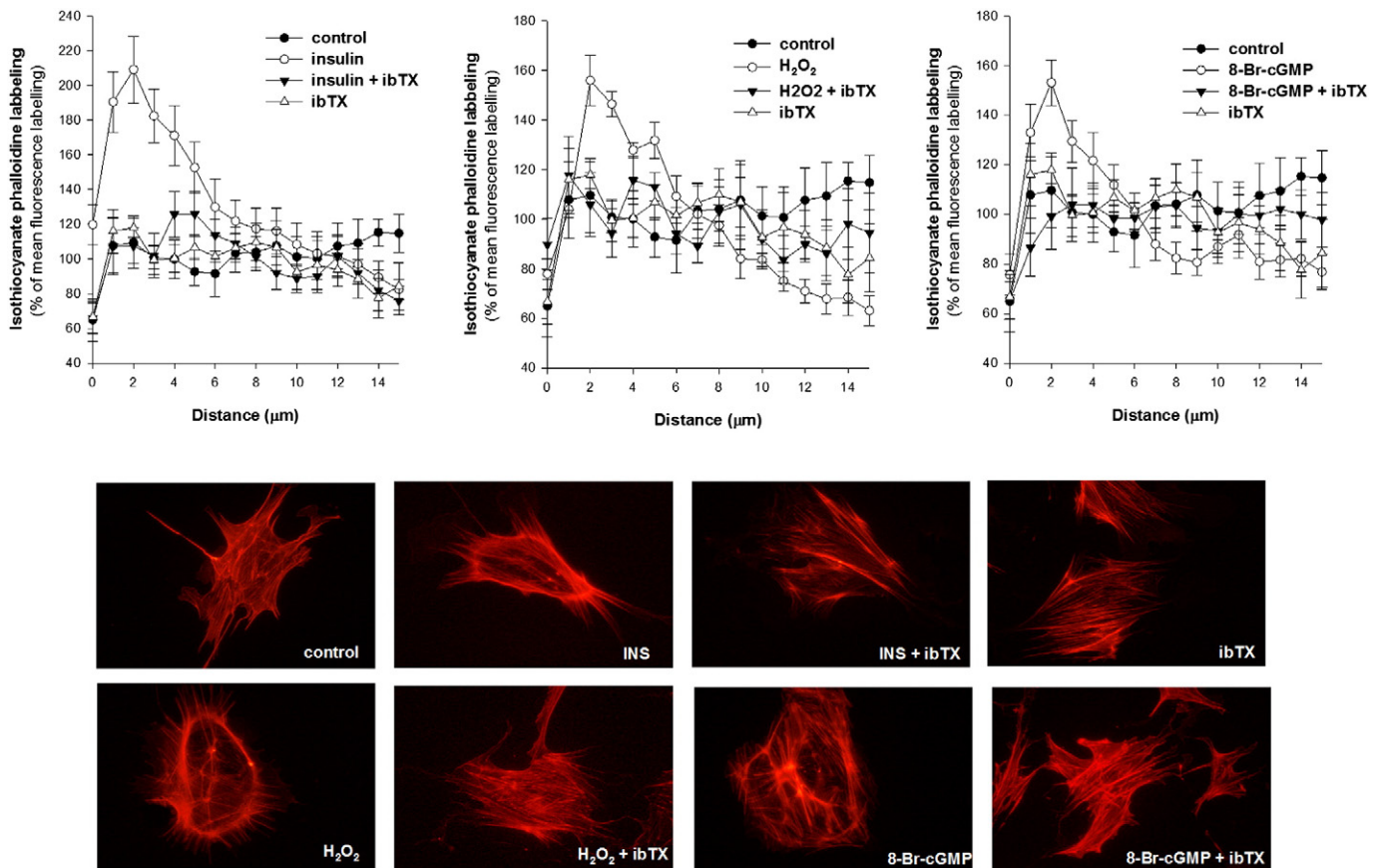


**Fig. 5.** Insulin remodels the actin cytoskeleton of podocytes via PKGα-dependent activation of the BK<sub>Ca</sub> channel. Rat podocytes were grown on coverslips, then incubated with insulin (300 nM, 5 min), PKG activators (H<sub>2</sub>O<sub>2</sub> and 8-Br-cGMP, 100 μM, 5 min), and the BK<sub>Ca</sub> inhibitor, iberitoxin (ibTX, 20 nM, 20 min). The F-actin network was labeled with isothiocyanate phalloidine and visualized with fluorescence microscopy. (Upper panel) The fluorescence intensity profile of the F-actin network. The digitized fluorescence images of the F-actin network were used to generate fluorescence intensity profiles (from the basal membrane to the nucleus) with CellSens imaging software. The values represent the mean ± SEM ( $n = 6-8$ ). (Lower panel) Representative images.

### 3.3. Insulin increases podocyte permeability to albumin via PKG $\alpha$ -dependent BK $_{Ca}$ mobilization

Fig. 3A shows that insulin significantly increased the permeability of a podocyte monolayer by about 81% (from  $52.87 \pm 3.1$  to  $95.86 \pm 7.39$ ,  $n = 4$ ). The PKG $\alpha$  activators, hydrogen peroxide and 8-Br-cGMP (both 100  $\mu$ M, 5 min) also increased podocyte permeability to albumin by about 134% and 112%, respectively. This effect was prevented by preincubations with the BK $_{Ca}$  inhibitor, iberiotoxin (20 nM, 20 min). We further investigated the role of the BK $_{Ca}$  channel in insulin-stimulated permeability to albumin by knocking-down BK $_{Ca}$   $\beta$  subunit expression with small-interfering RNAs (siRNAs). We found a significant reduction in MaxiK $\beta$  protein expression in podocytes transfected with MaxiK $\beta$  siRNA compared to cells transfected with scrambled siRNA (44.3% decrease compared to control,  $P < 0.05$ , Fig. 3B). Non-silencing siRNA (scrambled control) had no effect on MaxiK $\beta$  expression in control cells. Downregulation of MaxiK $\beta$  abolished the insulin-evoked increase in albumin permeation across the podocyte monolayer (Fig. 3C).

### 3.4. Insulin-induced phosphorylation of MYPT1 and RhoA kinase leads to actin reorganization through PKG $\alpha$ -dependent BK $_{Ca}$ activation in cultured rat podocytes

The PKG $\alpha$  isoform induces phosphorylation of MYPT1 at serine 695, which activates MLCP, and leads to a reduction in MLC phosphorylation. PKG $\alpha$  also induces phosphorylation of RhoA at serine 188, which leads to a reduction of RhoA kinase activity. We hypothesized that insulin could induce changes in MYPT1 and RhoA phosphorylation by activating PKG $\alpha$ , and that this signaling pathway required BK $_{Ca}$  activation.

To test this hypothesis, podocytes were incubated with insulin (300 nM, 5 min) and PKGI activators (8-Br-cGMP and H<sub>2</sub>O<sub>2</sub>, 100  $\mu$ M, 5 min) in the presence or absence of the BK $_{Ca}$  inhibitor, iberiotoxin (20 nM, 20 min). The cells were then lysed and the proteins analyzed by immunoblotting with anti-MYPT1, anti-p-MYPT1 (Ser 695), anti-RhoA, or anti-p-RhoA (Ser 188) antibodies. Insulin treatment increased the basal level of phosphorylated MYPT1 by 123% (from  $0.32 \pm 0.02$  to  $0.72 \pm 0.11$ ;  $P < 0.05$ , Fig. 4A) and increased the basal level of phosphorylated RhoA by 107% (from  $0.14 \pm 0.02$  to  $0.28 \pm 0.04$ ,  $P < 0.05$ , Fig. 4B). Both PKGI activators also increased phosphorylation of MYPT1 and RhoA in podocytes (Fig. 4A, B). The effects of insulin and the PKGI activators were abolished by preincubating cells with the BK $_{Ca}$  inhibitor (Fig. 4A, B,  $n = 4$ ,  $P < 0.05$ ).

Downregulation of MaxiK $\beta$  with small-interfering RNA (siRNA) also abolished the insulin-dependent increase in MYPT1 (Fig. 4C) and RhoA (Fig. 4D) phosphorylation.

The quantitative analysis confirmed that insulin and PKG $\alpha$  activators directly increased F-actin immunostaining in the vicinity of the plasma membrane, but had little effect on intracellular F-actin staining (Figs. 5,6). The effects of insulin and the PKGI activators on the F-actin network were abolished by preincubating with the BK $_{Ca}$  inhibitor (Fig. 5). These results suggested that insulin may regulate the contraction apparatus in podocytes via PKG $\alpha$ -dependent BK $_{Ca}$  channel activation.

### 3.5. The role of insulin in PKG $\alpha$ interactions with the Slo1 subunit of the BK $_{Ca}$ channel

Here, we addressed whether PKG $\alpha$  could associate with the BK $_{Ca}$  channel in rat cultured podocytes, and the role of insulin in this

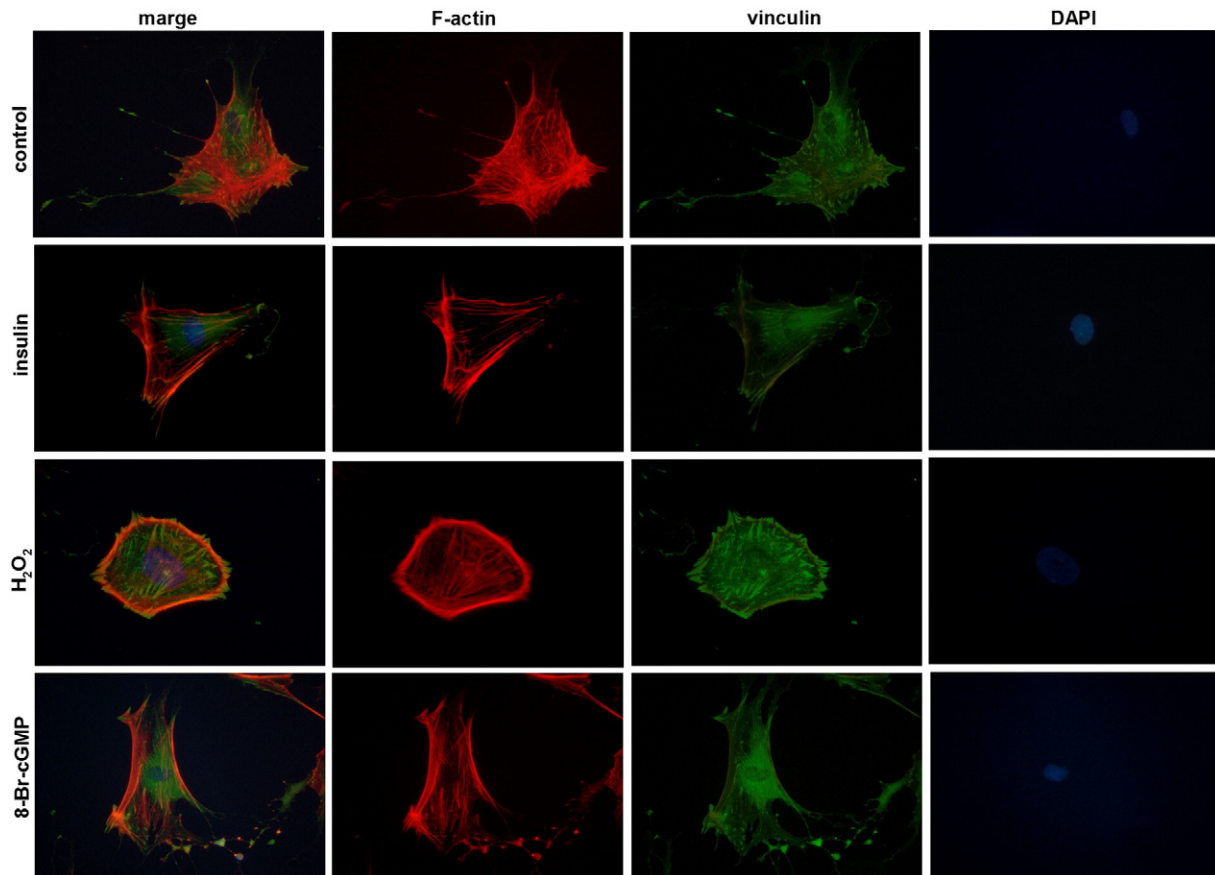


**Fig. 6.** Insulin and PKG activators remodel the actin cytoskeleton of podocytes. Rat podocytes were grown on coverslips, then incubated with insulin (300 nM, 5 min), PKG activators (H<sub>2</sub>O<sub>2</sub> and 8-Br-cGMP, 100  $\mu$ M, 5 min). F-actin network was labeled using isothiocyanate phalloidin, focal contacts were revealed using anti-vinculin monoclonal antibody and an Alexa488-conjugated secondary antibody, nuclear counterstaining revealed with DAPI.

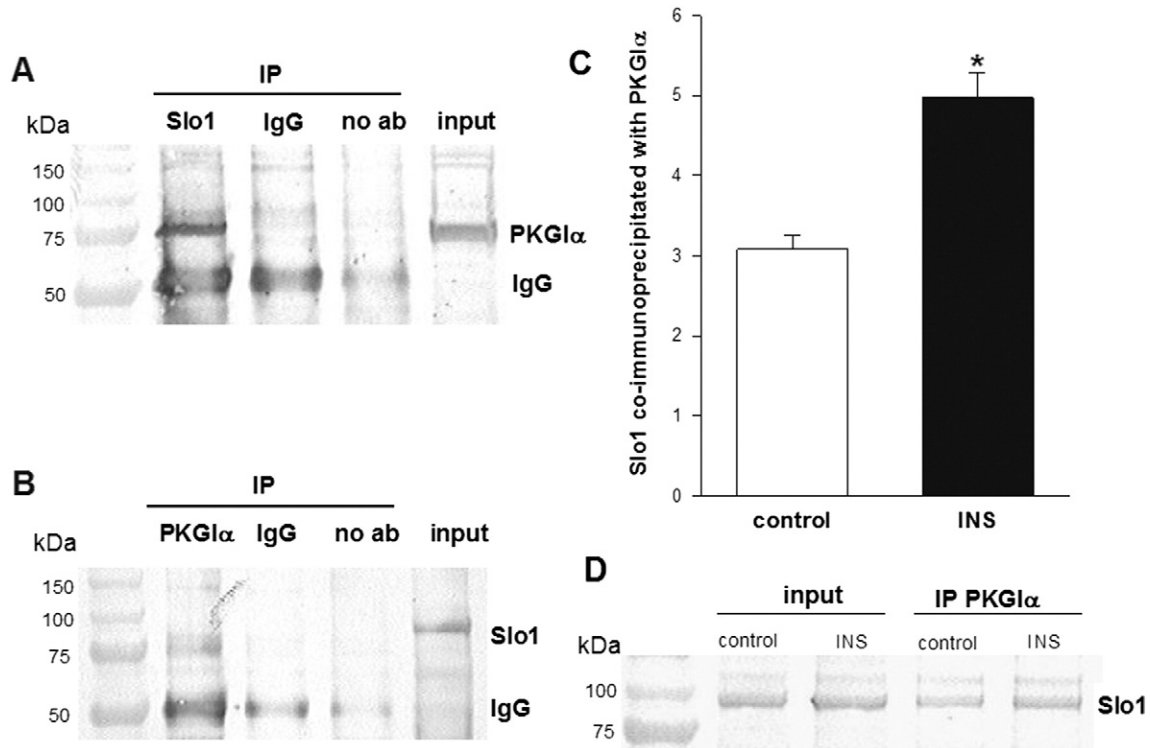


**Fig. 7.** PKGI $\alpha$  binds to large-conductance Ca<sup>2+</sup>-activated K<sup>+</sup> channel subunits. (A) Immunoblot shows that PKGI $\alpha$  was associated with the immunoprecipitated Slo1-subunit of BKCa in rat podocyte extracts. The input lane indicates a sample of the original cell lysate (before immunoprecipitation) from podocytes. (B) Immunoblot shows that the Slo1-subunit of BKCa was associated with the immunoprecipitated PKGI $\alpha$  in rat podocyte extracts. (C) Insulin increased the amount of Slo1 that was co-immunoprecipitated with PKGI $\alpha$ . Values represent the mean  $\pm$  SEM (n = 4). \*P < 0.05 compared to control; no ab: no antibody (negative control).

interaction. When podocyte extracts were mixed with a monoclonal antibody against the pore-forming subunit of BKCa, Slo1, PKGI $\alpha$  was detected in the immunoprecipitates (Fig. 7A). In the reciprocal procedure, where PKGI $\alpha$  was immunoprecipitated, the same interaction was observed (Fig. 7B). Moreover, the interaction was not observed in either direction when the immunoprecipitation was carried out without an antibody or when the antibody was preabsorbed with the appropriate antigen. The amount of Slo1 subunit that coprecipitated with PKGI $\alpha$  increased in the presence of insulin by about 61.4% (from  $3.08 \pm 0.17$  to  $4.97 \pm 0.31$ , n = 4, P < 0.05).

### 3.6. PKGI signaling affected insulin-dependent expression and membrane translocation of the Slo1 subunit of BKCa channels

Next, we investigated the translocation of the Slo1 subunit to the membrane in the presence of insulin (300 nM, 5 min) and/or the PKGI inhibitor, Rp-8-cGMPs (100  $\mu$ M, 20 min). Fig. 8 shows that insulin markedly enhanced the Slo1 subunit content in the membrane fraction, by about 132% (P < 0.05). Concomitantly, Slo1 content decreased in the cytosolic fraction, by about 30% (P < 0.05). These effects were abolished by pre-incubating podocytes with the PKGI inhibitor.

Immunofluorescence experiments showed that insulin and PKG activators (hydrogen peroxide and 8-Br-cGMP) caused substantial changes in the subcellular localization of the Slo1 subunit in cultured rat podocytes (Fig. 9). With insulin and PKG activators the intensity of Slo1 immunostaining increased close to the cell surface. Thus, insulin stimulation was associated with the translocation of the Slo1 subunit of the BKCa channel to the cell membrane via a PKGI-dependent mechanism.

## 4. Discussion

This study revealed a novel mechanism for insulin-mediated regulation of filtration barrier permeability via PKGI activation of BKCa

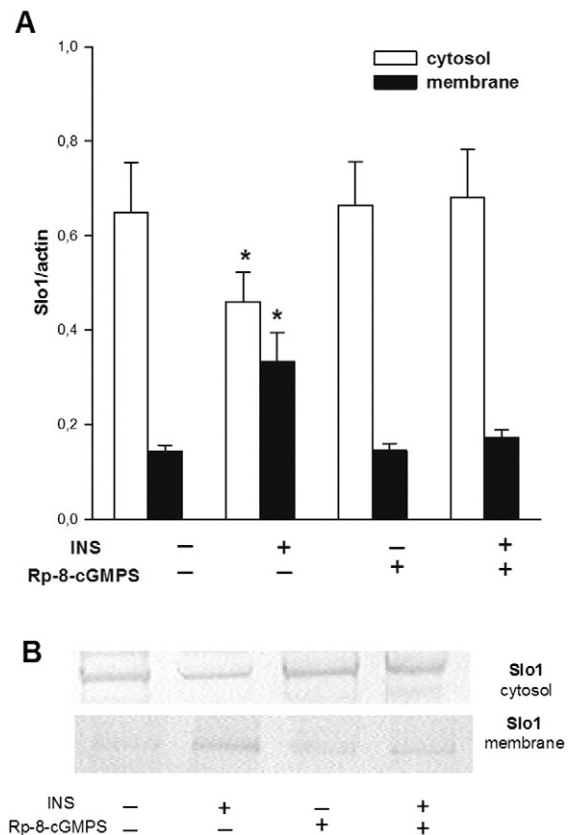


**Fig. 8.** Effect of PKGI $\alpha$  signaling on the expression and translocation of the Slo1 subunit. (A) Western blot analysis of cytosolic and membrane fractions. Values are the means  $\pm$  SEM (n = 4). \*P < 0.05 vs. control. (B) Representative immunoblots for cytosolic and membrane fractions.

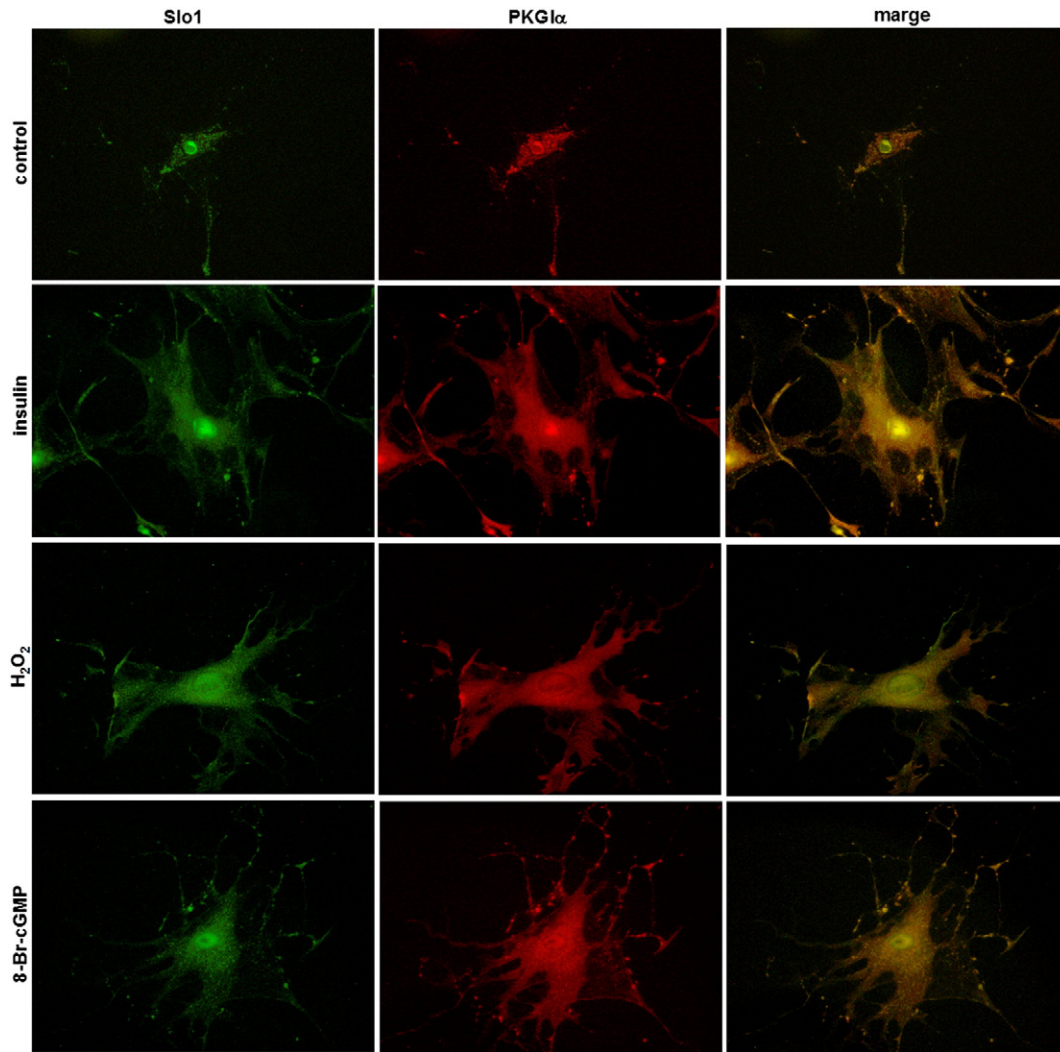


**Fig. 9.** Activation of PKGI $\alpha$  signaling pathways induced changes in subcellular distributions of PKGI $\alpha$  and the Slo1 subunit of the BK $_{Ca}$  channel. Rat podocytes seeded onto coverslips were incubated for 5 min in the absence or presence of 300 nM insulin, 100  $\mu$ M H $_2$ O $_2$ , or 100  $\mu$ M 8-Br-cGMP. Cells were then immunostained with anti-PKGI $\alpha$  and anti-Slo1 antibodies, as indicated.

channels in cultured rat podocytes. First, exogenous insulin induced an increase in albumin permeability and actin cytoskeleton reorganization, and both were dependent on BK $_{Ca}$  channel activation *via* PKGI. Second, insulin regulated the PKGI $\alpha$  interaction with the Slo1 subunit of the BK $_{Ca}$  channel; in addition, insulin regulated Slo1 expression on the cell surface *via* PKGI-dependent signaling in rat cultured podocytes.

Podocytes play an important role in determining the glomerular filtration rate (GFR) and in blocking the filtration of proteins [4]. Moreover, these cells have contractile activity, and they can respond to changes in glomerular capillary pressure [27]. A consistent finding was that insulin increased the GFR in insulin-sensitive subjects. This occurred through local renal vasodilation, which was mediated by a prostaglandin-dependent pathway [28] and regulated by endothelial NO synthase [29]. Interestingly, a number of groups have shown that insulin increased the GFR in subjects with normal insulin sensitivity, but this response was lost in insulin-resistant subjects [30, 31]. However, to date, the mechanism underlying this action has remained unknown.

In the present study, we assessed whether insulin-dependent effects on glomerular permeability to albumin were influenced by BK $_{Ca}$  inhibition. We used an *ex vivo* system of isolated glomeruli, because it allowed detection of rapid, subtle changes in albumin permeability without the influence of hemodynamics (changes in GFR) or circulating factors

(cytokines). Recently, we demonstrated that insulin increased albumin permeability in glomeruli isolated from Wistar rats by activating PKGI $\alpha$  [21]. The present study demonstrated that inhibition of BK $_{Ca}$  channels abolished that effect. We also found that the insulin effect on albumin permeability was evident in a cultured rat podocyte monolayer, and this effect was also dependent on BK $_{Ca}$  channel mobilization. Other authors previously demonstrated that the C-terminus of the human BK $_{Ca}$  channel  $\alpha$ -subunit enhanced the permeability of brain endothelial cells by interacting with caveolin-1 [32]. Moreover, we showed that podocyte permeability changed with PKGI $\alpha$  activators (8-Br-cGMP and hydrogen peroxide), and this effect was inhibited with a BK $_{Ca}$  channel inhibitor or after knocking-down BK $_{Ca}$  channel expression with siRNA. These results suggested that insulin increased albumin permeability across the podocyte filtration barrier through PKGI $\alpha$ -dependent, BK $_{Ca}$  channel activation.

In this study, we also showed that insulin regulated the contraction apparatus in podocytes *via* the PKGI $\alpha$ -dependent, BK $_{Ca}$  channel activation pathway. Previous studies have shown that PKGI mediated relaxation by acting on constriction apparatus proteins. MLCK increased cell constriction by phosphorylating MLC at Ser-19; conversely, relaxation was observed when MLCP was activated. PKGI $\alpha$  interacted directly with MYPT1 (which regulates MLCP) and that interaction led to reduced phosphorylation of MLC [10,33]. Recently, we also demonstrated that

insulin may induce changes in MYPT1 and MLC phosphorylation by activating PKG $\alpha$  [21].

Actin organization is regulated through the Rho kinase pathways [34]. One previous study showed that inhibition of Rho kinase led to time-dependent increases in flux through the podocyte barrier [35]. Those authors suggested that regulation of the actin cytoskeleton by Rho was critical for podocyte structure and permeability. Interestingly, PKG $\alpha$  had an inhibitory effect on Rho kinase activity [13]. In this study, we showed that insulin-mediated activation of PKG $\alpha$  caused an increase in the phosphorylation of RhoA kinase at position Ser188. These effects were abolished in the presence of a BK $_{Ca}$  channel inhibitor or after knocking-down BK $_{Ca}$  channel expression with siRNA. We hypothesized that insulin-induced changes in the contraction apparatus would require the activation of the BK $_{Ca}$  channel in rat cultured podocytes. Other authors have shown that BK $_{Ca}$  channel activity was reduced in microvascular smooth muscle cells isolated from insulin-resistant rats, which could impair vascular relaxation [36]. Collectively, these results revealed the critical importance of podocyte insulin sensitivity for kidney function.

We also showed that PKG $\alpha$  played a role in regulating the surface expression of the Slo1 subunit of BK $_{Ca}$  channels in podocytes. We showed that insulin markedly enhanced the Slo1 subunit content in the membrane fraction and concomitantly decreased the Slo1 content in the cytosolic fraction. Pre-incubating podocytes with a PKGI inhibitor abolished this effect. This study was the first to demonstrate that PKG $\alpha$  could interact with the Slo1 protein in rat cultured podocytes. Moreover, the amounts of Slo1 subunit that coprecipitated with PKG $\alpha$  increased in the presence of insulin. Other authors have also shown that insulin stimulated the expression of the Slo1 subunit of BK $_{Ca}$  channels in mouse podocyte plasma membranes. Insulin can also modulate BK $_{Ca}$  channel activity by activating the Erk/MAP kinase and PI3K/Akt signaling cascades [19]. It has been shown that nephrin can interact with the Slo1 and  $\beta$ 4 subunits of BK $_{Ca}$  channels, and that nephrin and actin dynamics are necessary for the normal expression of functional BK $_{Ca}$  channels on the podocyte cell surface [15,17]. Insulin also stimulated BK $_{Ca}$  channel activity in mesangial cells through a MAPK-dependent pathway; this pathway may also entail increased expression on the cell surface [37].

In summary, this study showed that insulin rapidly and directly stimulated signaling in the podocyte in the glomerulus. This signal could dynamically remodel the actin cytoskeleton of the podocyte to increase glomerular barrier permeability. We also showed that BK $_{Ca}$  played a critically important role in this process. This molecular mechanism might explain podocyte injury and proteinuria in diabetes.

#### Transparency documents

The Transparency documents associated with this article can be found, in online version.

#### Acknowledgements

This work was supported by grants from the National Science Center (2012/05/B/NZ4/02587) and from the Foundation for Polish Science (POMOST/2011-4/6).

#### References

- [1] H. Pavenstädt, W. Kriz, M. Kretzler, Cell biology of the glomerular podocyte, *Physiol. Rev.* 83 (1) (2003) 253–307.
- [2] H. Holthöfer, H. Ahola, M.L. Solin, S. Wang, T. Palmén, P. Luimula, A. Miettinen, D. Kerjaschki, Nephrin localizes at the podocyte filtration slit area and is characteristically spliced in the human kidney, *Am. J. Pathol.* 155 (1999) 1681–1687.
- [3] M.A. Saleem, L. Ni, I. Witherden, K. Tryggvason, V. Ruotsalainen, P. Mundel, P.W. Mathieson, Co-localization of nephrin, podocin, and the actin cytoskeleton: evidence for a role in podocyte foot process formation, *Am. J. Pathol.* 161 (2002) 1459–1466.
- [4] M.J. Morton, K. Hutchinson, P.W. Mathieson, I.R. Witherden, M.A. Saleem, M. Hunter, Human podocytes possess a stretch-sensitive, Ca $^{2+}$ -activated K $^{+}$  channel: potential implications for the control of glomerular filtration, *J. Am. Soc. Nephrol.* 15 (2004) 2981–2987.
- [5] A. Greka, P. Mundel, Balancing calcium signals through TRPC5 and TRPC6 in podocytes, *J. Am. Soc. Nephrol.* 22 (11) (2011) 1969–1980.
- [6] D. Drenckhahn, R.P. Franke, Ultrastructural organization of contractile and cytoskeletal proteins in glomerular podocytes of chicken, rat, and man, *Lab. Investig.* 59 (1988) 673–682.
- [7] M.A. Saleem, J. Zavadil, M. Bailly, K. McGee, I.R. Witherden, H. Pavenstädt, H. Hsu, J. Sanday, S.C. Satchell, R. Lennon, L. Ni, E.P. Bottinger, P. Mundel, P.W. Mathieson, The molecular and functional phenotype of glomerular podocytes reveals key features of contractile smooth muscle cells, *Am. J. Physiol. Renal Physiol.* 295 (2008) F959–F970.
- [8] N. Endlich, K.R. Kress, J. Reiser, D. Uttenweiler, W. Kriz, P. Mundel, K. Endlich, Podocytes respond to mechanical stress *in vitro*, *J. Am. Soc. Nephrol.* 12 (3) (2001) 413–422.
- [9] R. Sharma, H.B. Lovell, T.B. Wiegmann, V.J. Savin, Vasoactive substances induce cytoskeletal changes in cultured rat glomerular epithelial cells, *J. Am. Soc. Nephrol.* 3 (1992) 1131–1138.
- [10] H.K. Surks, N. Mochizuki, Y. Kasai, S.P. Georgescu, K.M. Tang, M. Ito, T.M. Lincoln, M.E. Mendelsohn, Regulation of myosin phosphatase by a specific interaction with cGMP-dependent protein kinase I alpha, *Science* 286 (1999) 1583–1587.
- [11] Y. Gao, A.D. Portugal, S. Negash, W. Zhou, L.D. Longo, J. Usha Raj, Role of Rho kinases in PKG-mediated relaxation of pulmonary arteries of fetal lambs exposed to chronic high altitude hypoxia, *Am. J. Physiol. Lung Cell. Mol. Physiol.* 292 (2007) L678–L684.
- [12] H.K. Surks, cGMP-dependent protein kinase I and smooth muscle relaxation: a tale of two isoforms, *Circ. Res.* 101 (2007) 1078–1080.
- [13] V. Sauzeau, H. Le Jeune, C. Cario-Toumaniantz, A. Smolenski, S.M. Lohmann, J. Bertoglio, P. Chardin, P. Pacaud, G. Loirand, Cyclic GMP-dependent protein kinase signaling pathway inhibits RhoA-induced Ca $^{2+}$  sensitization of contraction in vascular smooth muscle, *J. Biol. Chem.* 275 (2000) 21722–21729.
- [14] J.D. Stockand, S.C. Sansom, Mechanism of activation by cGMP-dependent protein kinase of large Ca(2+)-activated K $^{+}$  channels in mesangial cells, *Am. J. Physiol.* 271 (1996) C1669–C1677.
- [15] E.Y. Kim, K.J. Choi, S.E. Dryer, Nephrin binds to the COOH terminus of a large-conductance Ca $^{2+}$ -activated K $^{+}$  channel isoform and regulates its expression on the cell surface, *Am. J. Physiol. Renal Physiol.* 295 (1) (2008) F235–F246.
- [16] E.Y. Kim, Y.H. Chiu, S.E. Dryer, Nephrin regulates steady-state surface expression of Slo1 Ca(2+)-activated K(+) channels: different effects in embryonic neurons and podocytes, *Am. J. Physiol. Cell Physiol.* 297 (6) (2009) C1379–C1388.
- [17] E.Y. Kim, J.M. Suh, Y.H. Chiu, S.E. Dryer, Regulation of podocyte BK(Ca) channels by synaptopodin, Rho, and actin microfilaments, *Am. J. Physiol. Renal Physiol.* 299 (3) (2010) F594–F604.
- [18] E.Y. Kim, C.P. Alvarez-Baron, S.E. Dryer, Canonical transient receptor potential channel (TRPC)3 and TRPC6 associate with large-conductance Ca $^{2+}$ -activated K $^{+}$  (BK $_{Ca}$ ) channels: role in BK $_{Ca}$  trafficking to the surface of cultured podocytes, *Mol. Pharmacol.* 75 (3) (2009) 466–477.
- [19] E.Y. Kim, S.E. Dryer, Effects of insulin and high glucose on mobilization of slo1 BK $_{Ca}$  channels in podocytes, *J. Cell. Physiol.* 226 (9) (2011) 2307–2315.
- [20] G.I. Welsh, L.J. Hale, V. Eremina, M. Jeansson, Y. Maezawa, R. Lennon, D.A. Pons, R.J. Owen, S.C. Satchell, M.J. Miles, C.J. Caunt, C.A. McArdle, H. Pavenstädt, J.M. Tavaré, A.M. Herzenberg, C.R. Kahn, P.W. Mathieson, S.E. Quaggin, M.A. Saleem, R.J. Coward, Insulin signaling to the glomerular podocyte is critical for normal kidney function, *Cell Metab.* 12 (4) (2010) 329–340.
- [21] A. Piwkowska, D. Rogacka, M. Kasztan, S. Angielski, M. Jankowski, Insulin increases glomerular filtration barrier permeability through dimerization of protein kinase G type I $\alpha$  subunits, *Biochim. Biophys. Acta* 1832 (6) (2013) 791–804.
- [22] A. Piwkowska, D. Rogacka, M. Jankowski, K. Kocbuch, S. Angielski, Hydrogen peroxide induces dimerization of protein kinase G type I $\alpha$  subunits and increases albumin permeability in cultured rat podocytes, *J. Cell. Physiol.* 227 (3) (2012) 1004–1016.
- [23] R.P. Misra, Isolation of glomeruli from mammalian kidneys by graded sieving, *Am. J. Clin. Pathol.* 58 (1972) 135–139.
- [24] D. Pubill, G. Dayanithi, C. Siatka, M. Andrés, M.N. Dufour, G. Guillon, C. Mendre, ATP induces intracellular calcium increases and actin cytoskeleton disaggregation via P2x receptors, *Cell Calcium* 29 (2001) 299–309.
- [25] T. Oshima, F.S. Laroux, L.L. Coe, Z. Morise, S. Kawachi, P. Bauer, M.B. Grisham, R.D. Specian, P. Carter, S. Jennings, D.N. Granger, T. Joh, J.S. Alexander, Interferon-gamma and interleukin-10 reciprocally regulate endothelial junction integrity and barrier function, *Microvasc. Res.* 61 (2001) 130–143.
- [26] V.J. Savin, R. Sharma, H.B. Lovell, D.J. Welling, Measurement of albumin reflection coefficient with isolated rat glomeruli, *J. Am. Soc. Nephrol.* 3 (6) (1992) 1260–1269.
- [27] W. Kriz, E. Hackenthal, R. Nobiling, T. Sakai, M. Elger, B. Hähnel, A role for podocytes to counteract capillary wall distension, *Kidney Int.* 45 (2) (1994) 369–376.
- [28] A.J. Cohen, D.M. McCarthy, J.S. Stoff, Direct hemodynamic effect of insulin in the isolated perfused kidney, *Am. J. Physiol.* 257 (4 Pt 2) (1989) F580–F585.
- [29] K. Hayashi, K. Fujiwara, K. Oka, T. Nagahama, H. Matsuda, T. Saruta, Effects of insulin on rat renal microvessels: studies in the isolated perfused hydronephrotic kidney, *Kidney Int.* 51 (5) (1997) 1507–1513.
- [30] J.C. ter Maaten, S.J. Bakker, E.H. Serné, P.M. ter Wee, A.J. Donker, R.O. Gans, Insulin's acute effects on glomerular filtration rate correlate with insulin sensitivity whereas insulin's acute effects on proximal tubular sodium reabsorption correlation with salt sensitivity in normal subjects, *Nephrol. Dial. Transplant.* 14 (10) (1999) 2357–2363.

- [31] B.J. Tucker, M.M. Mendonca, R.C. Blantz, Contrasting effects of acute insulin infusion on renal function in awake nondiabetic and diabetic rats, *J. Am. Soc. Nephrol.* 3 (10) (1993) 1686–1693.
- [32] Y. Song, P. Wang, J. Ma, Y. Xue, C-terminus of human BK<sub>Ca</sub> channel alpha subunit enhances the permeability of the brain endothelial cells by interacting with caveolin-1 and triggering caveolin-1 intracellular trafficking, *Neurochem. Res.* 39 (2) (2014) 499–509.
- [33] K. Nakamura, Y. Koga, H. Sakai, K. Homma, M. Ikebe, cGMP-dependent relaxation of smooth muscle is coupled with the change in the phosphorylation of myosin phosphatase, *Circ. Res.* 101 (7) (2007) 712–722.
- [34] S. Etienne-Manneville, A. Hall, Rho GTPases in cell biology, *Nature* 420 (2002) 629–635.
- [35] J.L. Hunt, M.R. Pollak, B.M. Denker, Cultured podocytes establish a size-selective barrier regulated by specific signaling pathways and demonstrate synchronized barrier assembly in a calcium switch model of junction formation, *J. Am. Soc. Nephrol.* 16 (2005) 1593–1602.
- [36] C. Dimitropoulou, G. Han, A.W. Miller, M. Molero, L.C. Fuchs, R.E. White, G.O. Carrier, Potassium (BK(Ca)) currents are reduced in microvascular smooth muscle cells from insulin-resistant rats, *Am. J. Physiol. Heart Circ. Physiol.* 282 (3) (2002) H908–H917.
- [37] R.M. Foutz, P.R. Grimm, S.C. Sansom, Insulin increases the activity of mesangial BK channels through MAPK signaling, *Am. J. Physiol. Renal Physiol.* 294 (6) (2008) F1465–F1472.